RSC Advances

ROYAL SOCIETY OF CHEMISTRY

www.rsc.org/advances

Cite this: DOI: 10.1039/c0xx00000x

www.rsc.org/xxxxxx

COMMUNICATION

Redox-Active Gold Nanoclusters Immobilized ZnO Nanorod Electrodes for Electrochemical Sensing Applications†

Green Baek,[†a] Prabhu Pandurangan,[†a] Eunsol Ko,[a] Yirong Mo*[b] and Dongil Lee*[a]

Well-defined composite electrodes were fabricated by combining redox-active Au_{25} nanoclusters with highly oriented ZnO nanorods. The structure and electrocatalytic activity of the composite electrodes were examined for the development of an amperometric sensor for alkaline phosphatase.

Over the past few years, atomically monodisperse, thiolate-stabilized gold nanoclusters containing a few to a few hundreds of gold atoms have been the focus of intense research in both frontiers of fundamental science and technological applications.[1] These clusters exhibit size-dependent optical, electrochemical, and catalytic properties that differ substantially from their bulk counterparts.[2] For example, Au_{25} clusters display characteristic voltammetric redox peaks, revealing a wide opening of a HOMO-LUMO gap.[3] In our previous studies, we showed that these redox-active Au_{25} clusters can be used as an effective redox mediator in electrochemical sensing of biologically relevant analytes, such as ascorbic acid, uric acid, and dopamine.[4]

Recently, ZnO nanostructures have attracted much interest in electrochemical biosensors due to their biocompatibility, chemical stability, and electron communicating ability.[5a] Their desired orientations with a high isoelectric point (~9.5) allow facile and strong binding of various biomolecules on their surfaces, making them an attractive matrix for biosensor applications.[5b] ZnO nanostructures formed on various substrate electrodes have been used for the detection of biomolecules such as glucose, α-fetoprotein and rheumatoid arthritis.[6] Hybrid nanocomposites of ZnO have also been explored for biosensors. ZnO films modified with a redox-active mediator such as toluidine blue were employed for the detection of NADH.[7] Whereas ZnO matrix provides biocompatible environment, the redox-active molecule immobilized on the ZnO surface acts as a mediator, allowing sensitive detection of NADH at a low overpotential. In these nanocomposites, however, the intrinsically toxic nature of such mediator appears to limit their wide use in biosensors.[8]

Gold nanoparticles have been widely employed in electrochemical biosensors due to their biocompatibility, high conductivity, and electrocatalytic activity.[9a] Gold nanoparticles dispersed in various substrates such as self-assembled monolayer, carbon paste and polymer matrices have been used for chemical and biological sensing.[9b] Gold nanoparticles grown on ZnO nanostructures also showed enhanced electrocatalytic activity towards the detection of glucose and hydrazine.[10] However, gold nanoparticles employed in these composites have been limitedly used to enhance the electrocatalytic activity of the composites and their redox mediating ability remains largely unexplored. In this work, we explore the possibility of utilizing a redox-active Au_{25} cluster as a mediator by immobilizing it on ZnO nanorods (NRs) for the determination of alkaline phosphatase (ALP), a common enzyme label in immunoassays.[11a] The quantitative determination of ALP is also of interest in the field of routine clinical analysis. The diseases of liver and bone such as Paget's disease, osteomalacia and hepatitis are known to be related with high levels of serum ALP.[11b] Thus, the rapid and sensitive determination of ALP is of high significance.

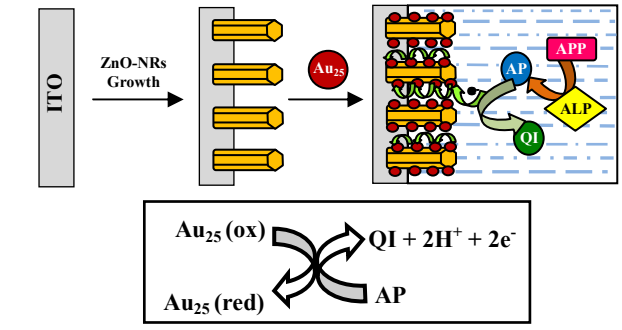

Scheme 1. Schematic of Au_{25}/ZnO/ITO electrode for the sensing of ALP by Au_{25}-mediated oxidation of AP to QI.

Highly oriented ZnO nanorods with average diameter of 150 nm and length of 1.5 μm were grown on indium tin oxide (ITO) electrode via a two-step solution process (ESI†).[12] Glutathione-stabilized Au_{25} clusters were synthesized according to a procedure[4b,13] described in ESI†. They display the characteristic UV-vis absorption profile of Au_{25} clusters[1] as shown in Fig. S1 (ESI†) and have a composition of Au_{25}(glutathione)$_{18}$ as confirmed by the negative-ion electrospray ionization (ESI) mass spectrum in Fig. S2 (ESI†). Four sets of peaks observed with m/z 1500-3000 represent 7-, 6-,

[a] *Department of Chemistry, Yonsei University, Seoul 120-749, Korea. E-mail: dongil@yonsei.ac.kr*

[b] *Department of Chemistry, Western Michigan University, Kalamazoo, Michigan 49008, USA. E-mail: yirong.mo@wmich.edu*

† Electronic supplementary information (ESI) available: Experimental, characterization and amperometric studies of Au_{25}/ZnO/ITO electrodes.

[†] These authors contributed equally to this work.

5-, and 4- anions of Au_{25}(glutathione)$_{18}$. The prepared ZnO/ITO electrode was then modified with glutathione-stabilized Au_{25} clusters by dropcasting an aqueous Au_{25} solution on the surface of ZnO nanorods and dried at 50 ^{o}C (Scheme 1). The glutathione ligand possesses two negatively charged carboxylate groups at a neutral pH (see Fig. S1 inset, ESI†). It is thus expected that glutathione-stabilized Au_{25} clusters electrostatically bind to the positively charged ZnO surface at a neutral pH. The fabrication procedure of Au_{25}/ZnO/ITO electrodes is described in ESI†.

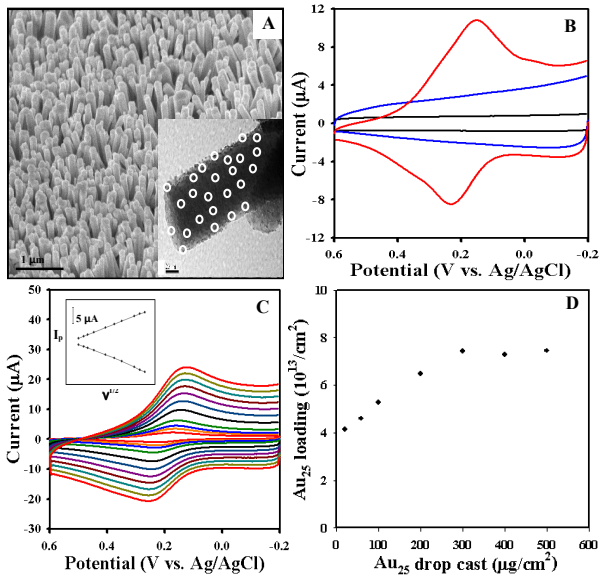

Fig. 1 (A) SEM image of Au_{25}/ZnO nanorods grown on ITO (scale bar = 1 μm); image taken at a 45^{o} tilt. Inset shows a TEM image (scale bar = 20 nm) of a single nanorod coated with Au_{25} clusters. Some of Au_{25} clusters are indicated with white circles. (B) CVs of bare ITO (black), ZnO/ITO (blue), and Au_{25}/ZnO/ITO (red) in 0.1 M KCl (pH = 7.0) at 50 mV/s. (C) CVs of Au_{25}/ZnO/ITO at varying scan rate (ν = 5-200 mV/s). Inset shows the plot of peak currents (I_p) vs. $\nu^{1/2}$. (D) Plot showing Au_{25} loading vs. Au_{25} amount dropcast on ZnO.

As shown in Fig. 1A, the image taken using a field-emission scanning electron microscope (SEM) shows that the entire ITO electrode is densely coated with highly uniform ZnO nanorods. In addition, the transmission electron microscopy (TEM) image in Fig. 1A inset shows that the ZnO surface is uniformly coated with Au_{25} clusters. The SEM energy dispersive spectrum (Fig. S3, ESI†) of the nanocomposite shows the presence of Au along with Zn, confirming stable immobilization of Au_{25} on ZnO nanorods.

In Fig. 1B, cyclic voltammograms (CVs) of bare ITO (black line) and ZnO/ITO electrode (blue line) in 0.1 M KCl show no distinct peak but only capacitive charging current. When ZnO/ITO electrode is modified with Au_{25} clusters, reversible anodic and cathodic peaks of Au_{25} are found at 0.23 and 0.17 V (vs. Ag/AgCl), respectively, that can be assigned to the redox peaks of Au_{25}. As observed before,[4a] the redox peaks of $Au_{25}^{+/0}$ and $Au_{25}^{0/-}$ couples are not well resolved in aqueous media presumably due to the high dielectric constant of the surrounding media. At any rate, the characteristic redox peaks of Au_{25} confirm that Au_{25} clusters are stably immobilized on ZnO nanorods and retain their redox activity. The effect of scan rate on the voltammetric response of the Au_{25}/ZnO/ITO electrode was examined in the range of 5 - 200 mV/s (Fig. 1C). The linear correlation of the peak currents (I_p) with square root of scan rates ($\nu^{1/2}$) suggests the voltammetric current response is controlled by the diffusion-like electron hopping process between Au_{25} clusters on ZnO surface.[4a]

The facile anchoring process of Au_{25} on ZnO enabled the control of Au_{25} loading by varying the amount of Au_{25} dropcast on ZnO surface. The Au_{25} loading on ZnO can be estimated by the integrated charge of the corresponding voltammetric peak. As can be seen in Fig. 1D, the Au_{25} loading increases with Au_{25} addition and levels off at around (~330 μg/cm^2). Beyond this concentration, Au_{25} clusters appear to be physically adsorbed but electrically unconnected to the ZnO/ITO electrode. The maximum Au_{25} loading was found to be ca. 8×10^{13} clusters/cm^2, which corresponds to ~8 full monolayers of Au_{25} on ITO substrate, showing that highly dense packing of Au_{25} can be achieved using ZnO nanorods.

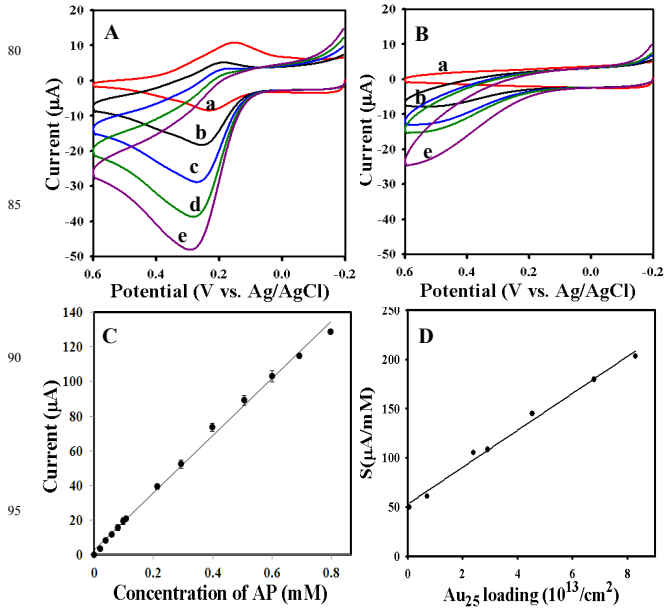

Fig. 2 CVs of (A) Au_{25}/ZnO/ITO and (B) ZnO/ITO electrode in the presence of 0, 0.05, 0.11, 0.17 and 0.23 mM AP (curves a to e) in 0.1 M KCl at 50 mV/s. (C) Calibration plot of current increase vs. AP concentration. (D) Plot of sensitivity (S) vs. Au_{25} loading.

ALP is known to hydrolyze a variety of orthophosphoric monoesters into the corresponding detectable phenol derivatives.[11a] We first examined the voltammetric response of the Au_{25}/ZnO/ITO electrode towards oxidation of p-aminophenol (AP), the end product of the enzymatic hydrolysis of p-aminophenylphosphate (APP) by ALP (Scheme 1). Fig. 2A shows CVs of Au_{25}/ZnO/ITO in the presence of 0, 0.05, 0.11, 0.17 and 0.23 mM of AP. The anodic peak currents significantly increase upon the addition of AP, indicating the mediated electrocatalytic activity of Au_{25}. As the potential is swept to the positive direction, Au_{25} is first oxidized. In the presence of AP the oxidized Au_{25} electrocatalytically oxidizes AP to

quinoneimine (QI) while it is reduced, as illustrated in Scheme 1. This process leads to enhancement of the anodic current of Au_{25}. The generated QI is rapidly hydrolyzed to p-benzoquinone and therefore only the increase in the anodic current is observed. For ZnO/ITO electrode (Fig. 2B), the oxidation of AP only occurs at a higher overpotential and the increment of current is much lesser than that observed for the Au_{25}/ZnO/ITO electrode.

The calibration graph shown in Fig. 2C shows the current response linearly increases with AP concentration in the range from 0.62 μM to 0.8 mM. The detection limit (S/N = 3) and the sensitivity were found to be 0.21 μM and 193.5 μA/mM, respectively. These values are comparable or better than those of recently reported electrochemical sensors for the determination of AP.[14] Evidently, the sensitivity increases with Au_{25} loading as can be seen in Fig. 2D. The sensitivity (determined in the range of 0.62-100 μM) for the composite electrode with Au_{25} loading of 0.05×10^{13} clusters/cm^2 was found to be 50.1 μA/mM. It increases linearly with Au_{25} loading and reaches to 203.4 μA/mM when the loading is increased to 8.3×10^{13} clusters/cm^2, confirming the role of Au_{25} in the detection of AP. The selectivity of the Au_{25}/ZnO/ITO electrode for the detection of AP was also investigated. The Au_{25}/ZnO/ITO electrode was found to exhibit some voltammetric response in the presence of potential interferents such as ascorbic acid and uric acid. To reduce the interference effect of these anions, the Au_{25}/ZnO/ITO electrode was coated with Nafion (1 vol% ethanol solution) and examined for the detection of AP in the presence of ascorbic acid and uric acid. As can be seen in Fig. S4 (ESI†) the Nafion coated electrode shows similar voltammetric oxidation and reduction peaks, but it shows much higher resistance to the addition of interferents; up to 240 μM and 150 μM for ascorbic acid and uric acid, respectively.

The detection of AP under dynamic condition was also examined by monitoring the chronoamperometric (CA) response of Au_{25}/ZnO/ITO electrode under stirring for the successive additions of AP with 60 s intervals at a fixed potential of 0.25 V as shown in Fig. S5 (ESI†). It was found from the amperogram and the calibration plot that this composite electrode exhibits an excellent linearity with enhanced sensitivity (247.8 μA/mM) for the determination of AP.

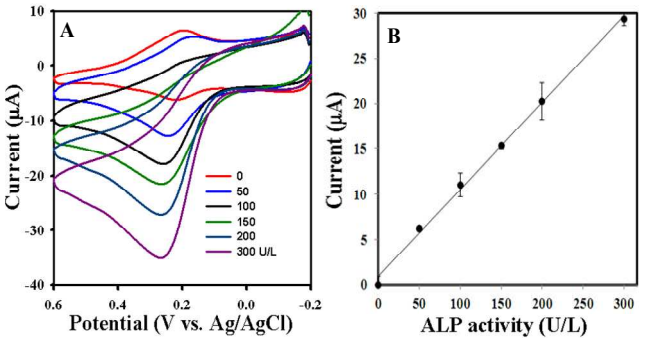

Fig.3 (A) CVs of Au_{25}/ZnO/ITO electrode upon the addition of ALP (after an incubation time of 5 min) obtained in the presence of 0.5 mM of APP in Tris-buffer (pH = 8.0) containing 0.1 M KCl and 1 mM $MgCl_2$ at 37°C. (B) Corresponding calibration curve for ALP.

The successful determination of AP with the Au_{25}/ZnO/ITO electrodes prompted us to directly determine the ALP activity as it rapidly hydrolyses APP to AP (Scheme 1). ALP is known to exhibit maximum activity at 37°C in the presence of Mg^{2+} that serves as an activator in basic media.[15] However, the electrostatic interaction between Au_{25} and ZnO becomes noticeably weakened above pH 9 and thus the determination of the ALP activity was conducted at pH 8 in the presence of 0.5 mM APP and 1 mM $MgCl_2$ at 37 °C. The change in CV upon the addition of ALP is shown in Fig. 3. The anodic current of Au_{25} increases linearly with ALP and the sensitivity for the determination of ALP was found to be 90.7 nAU^{-1}L. It is noteworthy that the detection potential of 0.25 V (vs. Ag/AgCl) with the composite electrode is much lower than those reported with screen printed graphite and micropatterned ITO electrodes for the determination of ALP.[11a, 16]

The time-dependent current response of the Au_{25}/ZnO/ITO composite electrode towards the detection of the ALP activity was also tested using CA in the range up to 300 U/L at 0.25 V. As shown in Fig. S6A (ESI†), the current response increases with ALP and the sensitivity determined from the initial slopes of the amperometric response curves was found to be 0.4925 nAs^{-1}U^{-1}L with a detection limit of 1.77 U/L (see Fig. S6B, ESI†). This sensitivity is more than 100 times higher than that reported for ALP sensing,[11a] enabled presumably by high electrocatalytic activity and dense packing of Au_{25} on ZnO nanorods. The current responses in Fig. S6A were found to be curved due to the depletion of AP during the amperometric measurement.

In summary, we have developed a highly sensitive electrochemical sensor by immobilizing redox-active Au_{25} clusters on ZnO nanorods. The high sensitivity could be realized by the excellent mediated electrocatalytic activity and dense loading of Au_{25} clusters on ZnO nanorods. With the unique size-dependent redox potentials, electrocatalytic activity and facile ligand engineering, the ultrasmall gold clusters immobilized on biocompatible ZnO nanostructures may prove useful in the development of biosensors and immunosensors.

This research was supported by Mid-Career Researcher Program (NRF-2011-0029735), Basic Science Research Program (NRF-2010-0009244), World Class University Program (R32-102170), and Priority Research Centers Program (20110022975) through the National Research Foundation of Korea (NRF) funded by the Ministry of Education, Science and Technology, and Yonsei University Research Fund.

Notes and references

1 H. Qian, M. Zhu, Z. Wu and R. Jin, *Acc. Chem. Res*., 2012, **45**,1470.

2 (a) H. Liu, X. Wu, X. Zhang, C. Burda and J.J. Zhu, *J. Phys. Chem. C*, 2012, **116**, 2548; (b) R. W. Murray, *Chem. Rev*., 2008, **108**, 2688; (c) Y. Zhu, H. Qian and R. Jin, *J. Mater. Chem*., 2011, **21**, 6793.

3 (a) D. Lee, R. L. Donkers , G. Wang, A. S. Harper and R. W. Murray, *J. Am. Chem. Soc*., 2004, **126**, 6193; (b) K. Kwak and D. Lee, *J. Phys. Chem. Lett*., 2012, **3**, 2476.

4 (a) S. S. Kumar, K. Kwak and D. Lee, *Anal. Chem.*, 2011, **83**, 3244; (b) K. Kwak, S. S. Kumar and D. Lee, *Nanoscale*, 2012, **4**, 4240.

5 (a) S. K. Arya, S. Saha, J. E. Ramirez-Vick, V. Gupta, S. Bhansali and S.P. Singh, *Anal. Chim. Acta*., 2012, **737**, 1; (b) F. Zhang, X. Wang, S. Ai, Z. Sun, Q. Wan, Z. Zhu, Y. Xian, L. Jin and K. Yamamoto, *Anal.*

Chim. Acta., 2004, **519**, 155.
6 (a) K. Yang, G.W. She, H. Wang, X. M. Ou, X. H. Zhang, C. S. Lee and S. T. Lee, *J. Phys. Chem. C*, 2009, **113**, 20169; (b) W. Hu, Y. Liu, H. Yang, X. Zhou and C. M. Li, *Biosens. Bioelectron*., 2011, **26**, 3683; (c) K. Y. Ahn, K. Kwon, J. Huh, G. T. Kim, E. B. Lee, D. Park and J. Lee, *Biosens. Bioelectron.*, 2011, **28**, 378.
7 S.A. Kumar and S. M. Chen, *Electroanalysis*, 2007, **19**, 1952.
8 C. V. Duijn Jr, *Experimental Cell Research*, 1962, **26,** 373.
9 (a) S. Guo and E. Wang, *Anal. Chim. Acta*., 2007, **598**, 181; (b) K. Sha, S. S. Agasti, C. Kim, X. Li and V. M. Rotello, *Chem. Rev*., 2012, **112**, 2739.
10 (a) Y. Wei, Y. Li, X. Liu, Y. Xian, G. Shi and L. Jin, *Biosens. Bioelectron*., 2010, **26**, 275; (b) C. Zhang, G. Wang, Y. Ji, M. Liu, Y. Feng, Z. Zhang and B. Fang, *Sens. Actuators B*, 2010, **150**, 247.
11 (a) R. E. Gyurcsányi, A. Bereczki, G. Nagy, M. R. Neuman and E. Lindner, *Analyst*, 2002, **127**, 235; (b) S. A. Rankin, A. Christiansen, W. Lee, D. S. Banavara and A. L. Hernandez, *J. Dairy Sci*., 2010, **93**, 5538.
12 (a) L. E. Greene, M. Law, D. H. Tan, M. Montano, J. Goldberger, G. Somorjai and P. Yang, *Nano Lett*., 2005, **5**, 1231; (b) L. E. Greene, B. D. Yuhas, M. Law, D. Zitoun and P. Yang, *Inorg. Chem*., 2006, **45**, 7535.
13. S. S. Kumar, K. Kwak and D. Lee, *Electroanalysis*, 2011, **23**, 2116.
14 (a) S. Ito, S. Yamazaki, K. Kano and T. Ikeda, *Anal. Chim. Acta*., 2000, **424**, 57; (b) A. Preechaworapun, Z. Dai, Y.Xiang, O. Chailapakul and J. Wang, *Talanta*, 2008, **76**, 424.
15 Md. R. Akanda, Md. A. Aziz, K. Jo, V. Tamilavan, M. H. Hyun, S. Kim and H. Yang, *Anal. Chem*., 2011, **83**, 3926.
16. H. J. Kim and J. Kwak, *J. Electroanal. Chem*., 2005, **577**, 243.

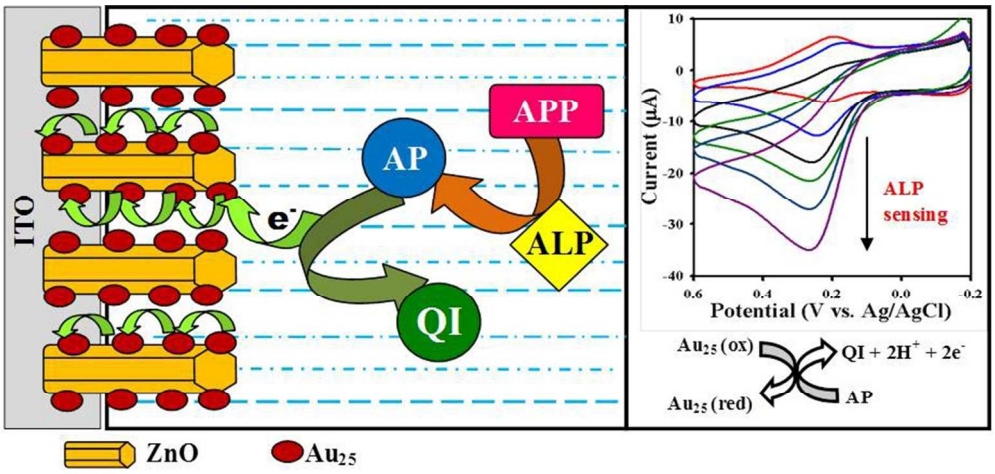

157x76mm (150 x 150 DPI)